J Biomol NMR (2010) 46:75–87
DOI 10.1007/s10858-009-9376-1

PERSPECTIVE

Methyl groups as probes of supra-molecular structure, dynamics and function

Amy M. Ruschak · Lewis E. Kay

Received: 20 August 2009 / Accepted: 9 September 2009 / Published online: 27 September 2009

Abstract The development of new protein labeling strategies, along with optimized experiments that exploit the label, have significantly impacted on the types of biochemical problems that can now be addressed by solution NMR spectroscopy. Here we describe how methyl labeling of key residues in a highly deuterated protein background has facilitated studies of the structure, dynamics and interactions of supra-molecular particles. The methyl-labeling approach is briefly reviewed, followed by a summary of applications to three different molecular machines so as to illustrate the types of questions that can now be addressed. Areas where future innovations will lead to yet further improvements are highlighted as well.

Keywords Aspartate transcarbamoylase · α-keto acids · Methyl group labeling · Methyl-TROSY · Proteasome · SecA

Introduction

Many of the accomplishments of biomolecular solution NMR spectroscopy can be credited to the emergence of double- and triple-resonance multi-dimensional methods that have greatly extended the range of problems that can be studied (Bax 1994). Using a variety of sophisticated experiments applied to biomolecules of ever-increasing complexity it has become possible to extract the chemical information of interest with site-specific resolution, often from a vast array of potentially interfering magnetic interactions. However, perhaps equally as important as the developed pulse schemes has been the concomitant improvement in isotopic labeling technologies that often drive the NMR methodology in the first place (Goto and Kay 2000; Kainosho et al. 2006). For example, early heteronuclear experiments focused on uniformly ^{15}N labeled protein samples and 3D ^{15}N-edited NOESY and TOCSY schemes (Marion et al. 1989). Subsequently, the uniform incorporation of ^{15}N and ^{13}C into protein molecules lead to the development of ^{15}N, ^{13}C, ^{1}H triple resonance experiments that facilitated studies of proteins in the 20–30 kDa molecular weight range (Ikura et al. 1990; Kay et al. 1990; Montelione and Wagner 1990). A further increase in the size of protein molecules that could be studied was realized by replacing many (or all) of the non-exchangeable proton spins by deuterons to produce ^{15}N, ^{13}C, ^{2}H-labeled proteins while retaining high levels of ^{1}H occupancy at backbone amide positions. Bax and coworkers first demonstrated the utility of combining triple-resonance methods with ^{2}H labeling/decoupling (Grzesiek et al. 1993), building on important studies in the 1960s by Crespi et al. (1968), Markley et al. (1968) and subsequently much later by LeMaster and Richards (1988) showing that deuteration leads to spectral simplification and to a marked improvement in the quality of ^{1}H NMR spectra. The reduction in relaxation rates for the remaining amide protons and for the aliphatic ^{13}C spins that are now one-bond coupled to deuterons had a very significant effect on increasing the size of proteins that could be investigated using triple-resonance approaches, as demonstrated by 'early' studies reporting the near complete backbone assignments of the *trp* repressor in its DNA-free (37 kDa) and DNA-bound (64 kDa) states (Shan et al. 1996; Yamazaki et al. 1994).

A. M. Ruschak · L. E. Kay (✉)
Departments of Molecular Genetics, Biochemistry and Chemistry, The University of Toronto, Toronto, ON M5S 1A8, Canada
e-mail: kay@bloch.med.utoronto.ca

However, the improved relaxation rates came at a price. The elimination of many of the aliphatic/aromatic protons that are responsible for a high fraction of the long range NOES in fully protonated proteins meant that structural studies of U-^{2}H labeled proteins would be significantly compromised. With this in mind some 15 years ago our laboratory initiated efforts to produce a labeling scheme which would retain a high level of deuteration, but would introduce a limited number of ^{1}H spins at key positions that could then serve as probes of both structure and dynamics. Our choice of methyl groups was based on a number of important factors. First, protein hydrophobic cores and protein–protein interfaces are typically enriched with methyls (Janin et al. 1988), and NOEs between methyl protons provide particularly useful structural restraints (Gardner et al. 1997; Metzler et al. 1996; Zheng et al. 2003). Second, since there are three protons per methyl group, methyl resonances are typically more intense than those from other moieties and they are also narrower due to rapid rotation about their three-fold axis and their location at the end of flexible amino acid side-chains (Nicholson et al. 1992; Tugarinov and Kay 2005a). Finally, although we did not realize it at the time, methyl groups are intrinsically optimized for use in TROSY spectroscopy (Pervushin et al. 1997), since in the limit of very rapid methyl rotation superimposed on the slow tumbling of a macromolecule, interference between dipolar interactions within the methyl group gives rise to classes of ^{13}C–^{1}H multiple quantum transitions that are immune to relaxation from intra-methyl dipolar fields, as well as to certain ^{1}H single-quantum transitions that relax independently of intra-methyl ^{1}H–^{1}H dipolar interactions (Tugarinov et al. 2003). Moreover, the simple HMQC experiment isolates the magnetization transfer pathway with these favorable relaxation properties from other less desirable pathways so that high sensitivity and resolution spectra can be recorded in a facile manner (Tugarinov et al. 2003).

A long period of trial and error in which a variety of different approaches for methyl labeling were attempted eventually lead to the use of α-keto acids as precursors for the production of methyl protonated Ile, Leu and Val residues in otherwise highly deuterated proteins (Gardner and Kay 1997; Goto et al. 1999). The utility of this labeling strategy for studies of the structure, dynamics and interactions of large proteins, including the 82 kDa enzyme malate synthase G (723 residues), has been the focus of a number of previous reviews (Tugarinov et al. 2004; Tugarinov and Kay 2005a), and our goal is not to repeat this here. Rather, in this review we briefly summarize the α-keto acid labeling strategy and further advances in methyl labeling that introduce methyl-protonated Ala residues and Met into deuterated proteins and then highlight the utility of this labeling strategy in concert with methyl-TROSY for studies of supra-molecular systems ranging in molecular weight from several hundreds of kDa to 1 MDa.

Production of methyl-labeled, highly deuterated proteins

Production of methyl labeled proteins can be achieved in a simple way through the addition of the appropriately labeled amino acids to a growth medium in which protein is over-expressed from a plasmid transformed most often into a standard strain of *E. coli* (Metzler et al. 1996). The main issues with this approach are cost and availability, although in recent years a wide variety of different amino acids have been synthesized as part of the SAIL strategy of protein labeling (Kainosho et al. 2006), see below. It is often the case, however, that amino acid precursors can be more easily generated that are then used to obtain the appropriately labeled proteins. For example, in an early reported description for the production of methyl labeled samples by Rosen et al. (Rosen et al. 1996), pyruvate was used as the carbon source. Protein expression in a D_2O based medium containing protonated pyruvate results in '$^{13}CH_3$ methyl labeling' for Ala, Val, Leu and Ile (γ2 only), with the majority of other positions deuterated. Unfortunately, protons in the methyl group of pyruvate exchange with deuterons in the solvent, leading to the production of additional methyl isotopomers (CH_2D, CHD_2, and CD_3), which are transferred to methyl groups of the biosynthesized protein. This is problematic for NMR applications, because each of the proton containing methyl isotopomers produces a separate correlation in ^{1}H–^{13}C spectra and the generation of CD_3 leads to a decrease in net signal intensity.

A better strategy, albeit one specific to Ile(δ1), Leu and Val, makes use of α-keto acids which are the direct biosynthetic precursors of these amino acids (and Met, see below). Specifically, α-ketobutyrate is the precursor for Ile (Gardner and Kay 1997), with the δ1 methyl group, the adjacent methylene, as well as the C^{α} and carbonyl carbons derived from this compound, Fig. 1a. α-ketoisovalerate is the precursor for both Leu and Val (Goto et al. 1999), determining the entire isotopic composition of both side chains, Fig. 1b, c. The α-keto acids are not sufficient as the only source of carbon in growth media because they are not involved in central metabolic pathways necessary for production of energy-storing molecules. Therefore, another carbon source must be provided, typically glucose, which determines the isotopic composition of the remaining carbon sites in the protein, including part of the Ile side chain (Fig. 1a), and the C^{α} and carbonyl carbons of Leu (Fig. 1b).

A large variety of isotopically labeled α-ketobutyrate and α-ketoisovalerate precursors are now available

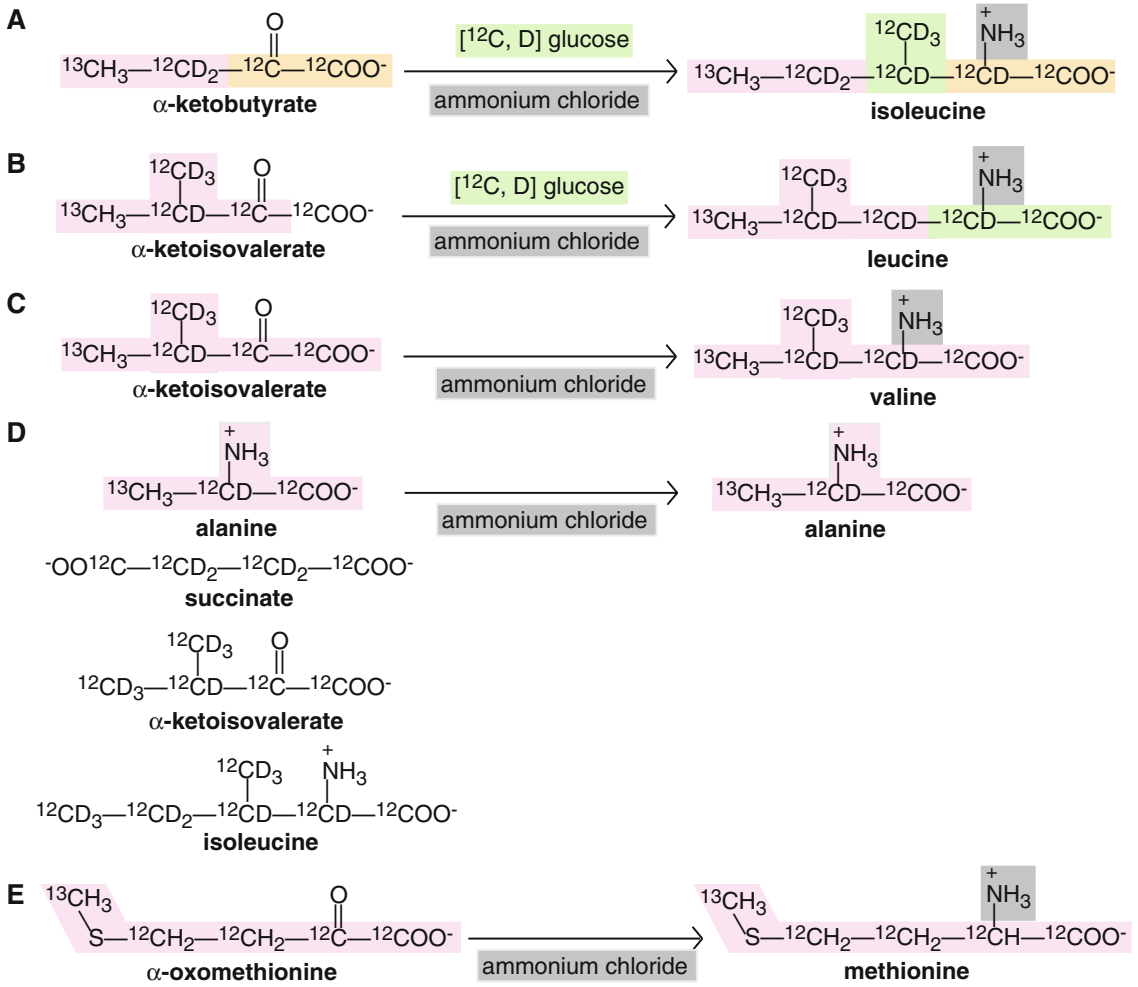

Fig. 1 Structures of biosynthetic precursors added to minimal media used to generate proteins with ^{13}C, ^{1}H labeled methyl groups of Ile (**a**), Leu (**b**), Val (**c**), Ala (**d**), and Met (**e**) in a ^{12}C, ^{2}H background. Coloring designates how each of the precursors, as well as glucose and ammonium chloride, become incorporated into each amino acid. Note for E, deuteration at the C^{γ} position (adjacent to S) could be achieved using formaldehyde-d_2 in the Barbier-type reaction used in the first step in the synthesis of α-oxomethionine (Fischer et al. 2007). The hydrogens at the carbon position adjacent to the carbonyl group are sufficiently acidic to be deuterated by incubation in D_2O at elevated pH. As an alternative to α-oxomethionine to generate methyl labeled methionine, the free methyl-labeled amino acid can also be added directly to protein expression media (Gelis et al. 2007)

commercially and their utility has been summarized previously (Tugarinov and Kay 2005a). In addition, efficient synthetic schemes for the production of these compounds have also appeared (Gross et al. 2003; Hajduk et al. 2000; Lichtenecker et al. 2004). Figure 1a–c shows versions of these compounds that are used for the production of highly deuterated proteins, with $^{13}CH_3$ labeling confined to methyl groups of Ile(δ1), Leu and Val (Tugarinov and Kay 2004). For studies of supra-molecular systems, in particular, it is necessary to minimize the number of protons so as to improve the relaxation properties of the methyl spins. Thus, [$^{13}CH_3$,$^{12}CD_3$]-α-ketoisovalerate is used, leading to Leu/Val residues with only a single 'NMR active' methyl group. Previous studies have shown that despite the fact that the number of methyl spins is decreased by a factor of two, the sensitivity of the Leu/Val region of correlation spectra is none-the-less improved, and the resolution far superior, for large proteins produced in this manner (Tugarinov and Kay 2004). It is worth mentioning that the isovalerate available commercially is a racemic mixture of pro-S and pro-R compounds, so that both methyls of the isopropyl moiety in Leu/Val are labeled, although only one per residue.

A strength of this labeling scheme is the ease of protein production. Ile(δ1), Leu, Val methyl labeled proteins are generated in a straightforward manner simply by the addition of α-ketoisovalerate ($\approx$90 mg/l) and α-ketobutyrate ($\approx$60 mg/l) 1 h prior to the induction of protein over-

expression (Goto et al. 1999). The production of highly deuterated, methyl protonated Ala labeled samples can also be accomplished through the addition of the appropriately labeled Ala, although a number of compounds must be added in this case to avoid scrambling of label, Fig. 1d (Ayala et al. 2009). A difficulty arises because Ala is produced directly as a result of transamination of pyruvate, which is also a precursor in the production of the branched-chain amino acids (Stryer 1995). This reaction is reversible so even if free methyl-labeled Ala is provided to the media, scrambling will occur with label incorporated at a variety of potentially undesired locations including methyl groups of Ile, Met, Leu, Thr and Val to levels as high as 25% (Ayala et al. 2009). Recently Boisbouvier and coworkers have developed a procedure to generate methyl labeling at Ala side chains with minimal (<1%) scrambling (Ayala et al. 2009). This was achieved by adding 2-[^{2}H],3-[^{13}C]-Ala (800 mg/l) as well as precursors for other pathways in which the scrambled amino acids are produced. Specifically, α-ketoisovalerate-d_7 (200 mg/l; suppresses scrambling to Leu, Val), succinate-d_4 (2.5 g/l; suppresses scrambling from pyruvate to many amino acids), and isoleucine-d_{10} (60 mg/l) are included in growth media. Another approach for the production of proteins with methyl-labeled Ala involves the addition of 3-^{13}C Ala (50 mg/l) to rich deuterated media (Isaacson et al. 2007), but the incorporation of labeled Ala is much lower using this procedure. Finally, it is worth noting that Met methyl groups are also very useful probes of supra-molecular structure and dynamics (Gelis et al. 2007), in particular since the often high mobility of such moieties ensures that narrow spectral linewidths are obtained. Labeling can be achieved through the addition of fully protonated $^{13}C^{\varepsilon}$-Met that is commercially available or via an α-keto acid derivative that can be synthesized via a scheme recently described (Fischer et al. 2007), Fig. 1e, offering the possibility of incorporation of deuterons into non-methyl positions.

As described above, in the past several years a large number of selectively labeled amino acids have become available and they can be incorporated into proteins via expression using a cell-free approach (Spirin et al. 1988). Cell free methods have been central to the development of complex isotope labeling methods such as SAIL (Kainosho et al. 2006) in which proteins are produced with fractionally protonated amino acids, with each residue containing a specific isotopomer composition. This method provides the labeling of choice for detailed structural studies of proteins with molecular weights in the 50–100 kDa regime, cost issues notwithstanding, although for applications to supra-molecular systems 'tailored methyl labeling' focusing on Ile, Leu, Val, Fig. 1a–c, as well as Ala, Fig. 1d, and Met, Fig. 1e, is preferred.

Applications to very high molecular weight particles

The goal

With the development of modern multi-dimensional protein NMR spectroscopy the emphasis shifted to the production of U-^{15}N, ^{13}C labeled proteins and the assignment of the great majority of ^{15}N, ^{13}C and ^{1}H spins as a prelude for in-depth structural studies (Clore and Gronenborn 1991). A wide array of triple-resonance experiments has been developed for achieving this goal (Sattler et al. 1999). The basic strategy that emerged early on in studies of relatively small proteins—assign as many sites as possible—essentially remained unchanged, even as studies progressed to molecules with molecular weights in the 40–50 kDa range where the sensitivity of many of the experiments becomes compromised. In applications to even larger systems the 'end-game' is different. Here the goal is to use either backbone amide (Fiaux et al. 2002; Kobayashi et al. 2008) or methyl group probes (Amero et al. 2009; Gelis et al. 2007; Hamel and Dahlquist 2005; Isaacson et al. 2007; Kreishman-Deitrick et al. 2005; Sprangers et al. 2005; Sprangers and Kay 2007b; Velyvis et al. 2007) to address specific questions of molecular function within the broader context of the biophysical information that is already available. Thus, the approach builds upon existing data and in this context NMR studies become very complementary to other more traditional approaches. Indeed, a pre-requisite for undertaking such studies is the availability of high resolution structures from X-ray diffraction or cryo-electron microscopy. In what follows a number of applications of the methyl-labeling approach to studies of molecular machines is described, illustrating the range of problems that are currently amenable to the technology and the insights that are made into supra-molecular structure, dynamics and function.

Aspartate transcarbamoylase

The first step in the biosynthesis of the pyrimidine nucleotides CTP and UTP is catalyzed by the allosteric enzyme aspartate transcarbamoylase, ATCase (Stryer 1995). This 300 kDa enzyme is an oligomer that is comprised of six catalytic (c) polypeptide chains, which contain the sites that catalyze the chemical reaction converting reactants carbamoyl phosphate and aspartate to products carbamoyl aspartate and phosphate, and six regulatory (r) polypeptide chains, which regulate the reaction through binding of small molecule effectors (Lipscomb 1994). Binding of aspartate causes a sigmoidal increase in the rate of enzyme function. This observation is best explained by the Monod–Wyman–Changeux (MWC) model of allostery which postulates that the enzyme exists in equilibrium between two states, T and R, with the latter having a higher affinity

for substrate (Monod et al. 1965). In this model the conformations of each of the chains within a given state are equivalent. Notably, the activity of ATCase is also controlled by nucleotides CTP and ATP, where binding of CTP to the r chains causes the activity of the enzyme to decrease, while ATP binding has the opposite effect (Schachman 1988). A number of models have been put forth to explain the allosteric effects of nucleotide binding on the catalytic sites located 60 Å away. It has been argued that the MWC model applies also for binding of ATP and CTP, with preferential binding to the R and T states, respectively (Eisenstein et al. 1990; Schachman 1988). An alternative model has also been proposed in which binding of nucleotide induces a conformational change in the catalytic site without a concomitant shift in the R/T equilibrium (Tauc et al. 1982; Thiry and Herve 1978). Methyl-TROSY studies are ideally suited to address this issue (Velyvis et al. 2007).

Figure 2a shows a region of the ^{13}C–^{1}H methyl-HMQC correlation map of U-^{2}H, Ile-[$\delta1^{13}CH_3$]-labeled WT ATCase (800 MHz, 37°C) to which saturating amounts of PAM (phosphonoacetamide), a non-hydrolyzable analogue of carbamoyl phosphate, and either ATP or CTP are added. A pair of peaks from a single Ile reporter is shown, derived from ATCase in either the T or R conformations that exchange slowly on the NMR chemical shift time-scale. The addition of ATP clearly shifts the R/T equilibrium towards R with the opposite effect occurring for CTP, consistent with the MWC model, Fig. 2a. A similar situation occurs when ATP is added to apo-ATCase, Fig. 2b. The T-state of the WT enzyme, which is the dominant state in the absence of ligands, shifts slightly to the R-form ($\approx$5%). These results argue unequivocally against any model postulating no change in the R/T equilibrium upon nucleotide binding (Velyvis et al. 2007). However, these findings do not exclude the possibility that ATP/CTP association results in both a shift in equilibrium and a change in structure at the catalytic sites. This question, like the issue of an equilibrium shift posed above, can also be answered by direct inspection of spectra of suitably labeled enzyme (Velyvis et al. 2009).

Figure 2c shows an overlay of ^{13}C–^{1}H HMQC spectra of U-^{2}H, Ile-[$\delta1^{13}CH_3$], Leu,Val-[$^{13}CH_3$,$^{12}CD_3$] c-chain, unlabeled r-chain ATCase (800 MHz, 37°C) in the absence (black) and presence (red) of saturating amounts of ATP. The absence of changes in chemical shifts argues strongly against structural changes to the c-chains upon ATP binding to the r-chains. Additional supporting data can be obtained in the form of ^{13}C–^{1}H methyl residual dipolar coupling values that have been measured on partially aligned ATCase samples labeled as described above (Velyvis et al. 2009). Each RDC provides a quantitative measure of the orientation of the bond vector connecting the $^{13}C_{methyl}$ and its attached carbon with respect to the unique axis of the threefold symmetric ATCase and as such is a very sensitive probe of structure. Accurate coupling measurements are obtained using a methyl-TROSY scheme (Sprangers and Kay 2007a) whereby each of the two methyl ^{1}H multiplet components that arises due to coupling with ^{13}C is separated into a pair of data sets by post-acquisition processing (Ottiger et al. 1998; Yang and Nagayama 1996), with the spacing between multiplets providing a measure of either J_{methyl} (no alignment) or $J_{methyl} + D_{methyl}$, Fig. 2d. The correlation between D_{methyl} values measured on samples of PAM-saturated ATCase in the presence (*Y*-axis) and absence (*X*-axis) of Na_2ATP is shown in Fig. 2e, with the corresponding correlation for Na_2CTP in Fig. 2f. Very high levels of correlation are obtained, with Pearson's correlation coefficients $R > 0.99$ in both cases; in the extremely unlikely event that the small RMSDs between RDC values measured for apo- and bound-states ($\approx$1 Hz) reflect actual structural differences and not experimental uncertainties in measurements, they must correspond to C^{α} RMSD differences of well under 0.2 Å (Velyvis et al. 2009). This level of correlation is consistent with expectations based on chemical shift data, Fig. 2c, and establishes that nucleotide binding does not affect the structure of the catalytic chain. Any model invoking such a structural change must therefore be incorrect.

It is important to note that insight into the mechanism of allostery in this 300 kDa system could be obtained without the time-consuming step of methyl chemical shift assignment simply by examining how NMR properties (chemical shifts, RDC values) change upon addition of allosteric effectors. Of course, in other applications site-specific information is required and here assignments are a prerequisite, as outlined below.

20S core particle proteasome

The 20S core particle (CP) proteasome is a 670 kDa protein complex that regulates cellular function by catalyzing the proteolysis of proteins that are either damaged or no longer needed (Pickart and Cohen 2004). Because of its importance in the cell it has emerged as a drug target in the fight against certain types of cancer (Adams 2004). Static pictures of the 20S CP proteasome have been obtained using X-ray crystallography (Forster et al. 2005; Lowe et al. 1995) and electron microscopy (Rabl et al. 2008), revealing a molecular machine built from a series of concentric, stacked rings, which form a hollow, cylindrical-shaped chamber (Fig. 3a). In the case of core particles isolated from archaea each of the outer (inner) rings is comprised of seven equivalent α- (β-) subunits, while in more complex organisms the subunits differ (Pickart and Cohen 2004). The N-termini of the α-subunits form gates that cap the two ends of this core structure (Cheng 2009) so

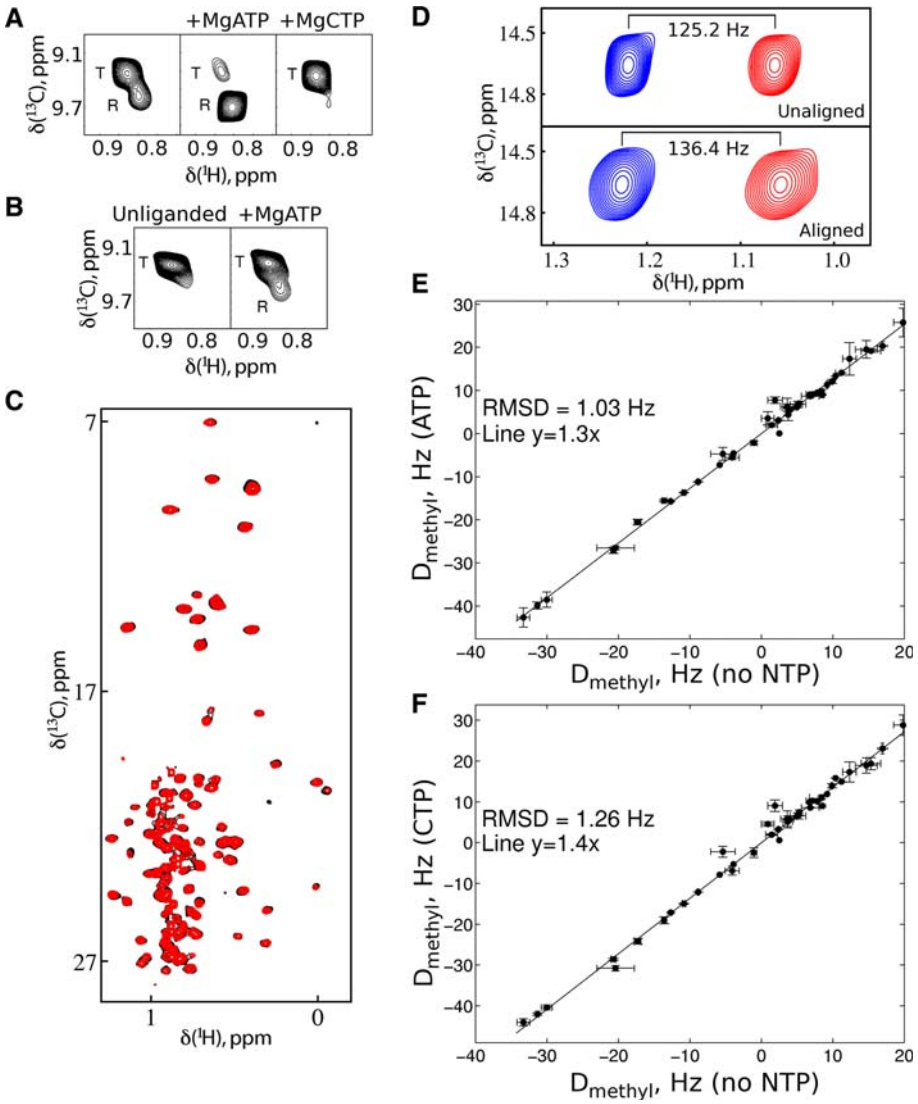

Fig. 2 Binding of ATP and CTP to ATCase (Velyvis et al. 2007, 2009). **a** Selected region of ^{13}C–^{1}H HMQC spectra of U-[^{2}H], Ile-[$\delta1^{13}CH_3$]-labeled WT ATCase, saturated with the substrate analog PAM (*left*). Peaks from the R and T enzyme conformations are indicated. The effects of saturating amounts of MgATP (*center*) and MgCTP (*right*) on the spectrum are also shown, indicating shifts towards the R and T states upon ATP and CTP binding, respectively. **b** ^{13}C–^{1}H correlation maps of unliganded WT ATCase, with isotopic labeling as in **a**, in the absence (*left*) or presence (*right*) of saturating amounts of MgATP. **c** ^{13}C–^{1}H HMQC spectrum of cK164E cE239K, PAM-bound ATCase in the absence (*black*) or presence (*red*) of 20 mM ATP recorded on a sample where the c-chain is Ile-[$\delta1^{13}CH_3$], Leu,Val-[$^{13}CH_3$,$^{12}CD_3$] labeled and the r-chain is unlabeled, indicating that nucleotide binding does not induce conformational changes to the c-chain. **d** Measurement of methyl ^{13}C–^{1}H RDC values on a sample of ATCase, Ile-[$\delta1^{13}CH_3$], Leu,Val-[$^{13}CH_3$,$^{12}CD_3$] labeled in the c-chain, unlabeled r-chain. Spectra were recorded in the absence (*top*) and presence (*bottom*) of alignment media, with the change in peak splitting upon introduction of alignment media (11.2 Hz) corresponding to D_{methyl} (see text). Correlations between D_{methyl} values measured on ATCase in the presence (*Y*-axis) and absence (X-axis) of ATP (**e**) or CTP (**f**), using samples described as in **d**. For both ATP and CTP the values of D_{methyl} in the presence of nucleotide are a factor of 1.3–1.4 larger in magnitude than without, indicating that ATCase in the nucleotide bound form aligns more strongly. Sections of this figure have been adapted from Velyvis et al. (2007, 2009)

that entry of proteins into the chamber for degradation is regulated. Although the insights obtained from the static 20S CP structures are extremely important, they do not inform on the time-dependent transient interactions and motions that are central to the function of this machine (Sprangers and Kay 2007b).

Because site-specific information is necessary to understand how dynamics might mediate function, chemical shift assignments of probes within the complex are critical. To this end, samples of 20S CP proteasome were prepared where the α-rings were labeled as U-^{2}H, Ile-[$\delta1^{13}CH_3$],Leu,Val-[$^{13}CH_3$,$^{12}CD_3$], with the β-rings

remaining unlabeled. In addition, a series of molecules were produced to 'assist' in the assignment process, including a monomeric version of the α subunit (20 kDa) in which a series of mutations were introduced to prevent oligimerization, and a 'half-proteasome' comprised of a pair of α_7 rings that stack on each other ($\alpha_7\alpha_7$, 360 kDa). Assignments for the α subunit were readily obtained using standard triple-resonance approaches and subsequently transferred to $\alpha_7\alpha_7$ and then to the 20S CP by comparing a series of 3D through-bond and NOE data sets that were recorded on the particles (Sprangers and Kay 2007b). The details of the 3D through-bond methodology have been reported in a series of publications (Tugarinov and Kay 2003a, b), with a number of small modifications to incorporate the methyl-TROSY effect (Sprangers and Kay 2007b). It is worth noting that, unlike the HMQC and NOESY data sets that are obtained on samples labeled as described above, the through-bond experiments were preformed on samples with U-^{13}C labeling with the exception of Leu and Val where the isopropyl methyl groups are of the [$^{13}CH_3$,$^{12}CD_3$] variety. This 'linearization' of side-chain spin systems is advantageous since magnetization can be transferred from the methyl ^{13}C spin to any specific carbon along the side-chain using a series of INEPT-based schemes that often leads to spectra with improved sensitivity relative to those where magnetization transfer occurs via a TOCSY approach (Tugarinov and Kay 2003b). In the case of Ile residues where it is not possible to use precursors that lead to a linearization of the spin system in a cost effective manner, the use of INEPT-based magnetization transfers that are selective in the sense that only certain ^{13}C–^{13}C couplings are allowed to evolve, leads to the directed flow of magnetization that optimizes sensitivity (Tugarinov and Kay 2003b). The majority of methyl assignments for the proteasome were obtained from the 'optimized' spectroscopy summarized above. However, it is worth mentioning that in a number of cases where assignments of correlations were not forthcoming from a comparison of 3D data they were obtained by mutagenesis.

With the availability of 90% of the Ile(δ1), Leu and Val methyl assignments for the α-rings of the 20S CP and over 95% of the assignments for $\alpha_7\alpha_7$ it becomes possible to obtain detailed site-specific dynamics information for the α-chain over a broad spectrum of time-scales (Sprangers and Kay 2007b). Initially NMR experiments were performed for quantifying fast, internal motions on the nano- to picosecond timescale, Fig. 3b. Values of the square of the methyl axis order parameter, S^2_{axis}, were obtained from separate ^{13}C and ^{2}H spin-relaxation experiments recorded on samples with $^{13}CHD_2$-labeled methyl groups (Tugarinov and Kay 2005b) and from ^{1}H-based relaxation experiments measured on $^{13}CH_3$ methyls (Tugarinov et al. 2007). The correlation between S^2_{axis} values obtained using the different approaches is very high, Fig. 3bi, validating the methodology. As expected, the distribution of S^2_{axis} values spans essentially the complete range from 0 to 1, indicating a wide range of mobilities that depend on the local environment, Fig. 3bii. Interestingly, a cluster of residues that are highly flexible ($S^2_{\text{axis}} < 0.3$) was identified on the outside of the alpha ring near the interface between alpha subunits (Fig. 3biii) (Sprangers and Kay 2007b). This highly mobile cluster carries a potential nuclear localization-type signal that binds to protein targets and it may be that the motional properties of this region are important for modulating the binding interactions.

Relaxation dispersion experiments exploiting the methyl-TROSY effect (Korzhnev et al. 2004) were carried out to probe millisecond (ms) time-scale dynamics, Fig. 3ci. Figure 3cii illustrates those regions of the α-rings for which a concerted, ms process was observed, with motion localized to the inside surface of much of the antechamber, including the entrance pores (red and yellow balls). Such dynamics may play a role in moderating interactions between unfolded ('sticky') substrates and the walls of the proteasome so as to facilitate efficient translocation of substrate into the catalytic chamber for degradation (Sprangers and Kay 2007b).

Methyl groups can also be used as probes of molecular interactions and chemical shift studies of the 20S CP with a number of targets, including the 11S activator, have been reported (Sprangers and Kay 2007b). A recent binding study of the inhibitor chloroquine to the proteasome revealed a new mode of proteasome–inhibitor interaction, in which chloroquine binds to a region distal from the active sites of the protease and through some still unknown mechanism is able to inhibit substrate proteolysis (Sprangers et al. 2008). The realization that proteasome activity can be modulated through inhibitors interacting at a variety of sites opens up the possibility of a 'multi-pronged' approach of inhibition that has proven to be successful in applications to other targets, such as the HIV protease. Indeed, an inhibitor with a structure related to cloroquine has recently entered phase 1 clinical trials (Mao et al. 2009).

SecA

SecA is a component of a membrane-bound protein complex that acts as a channel to transport newly synthesized proteins across bacterial and chloroplast membranes. There are two roles that SecA plays in this process, including substrate recognition for translocation (Wang et al. 2000), and providing the energy for insertion of substrate into the membrane via ATP hydrolysis (Driessen et al. 1991; Economou and Wickner 1994; Matsumoto et al. 1997). Although it is clear that recognition by SecA occurs via a signaling sequence at the N-termini of substrate molecules

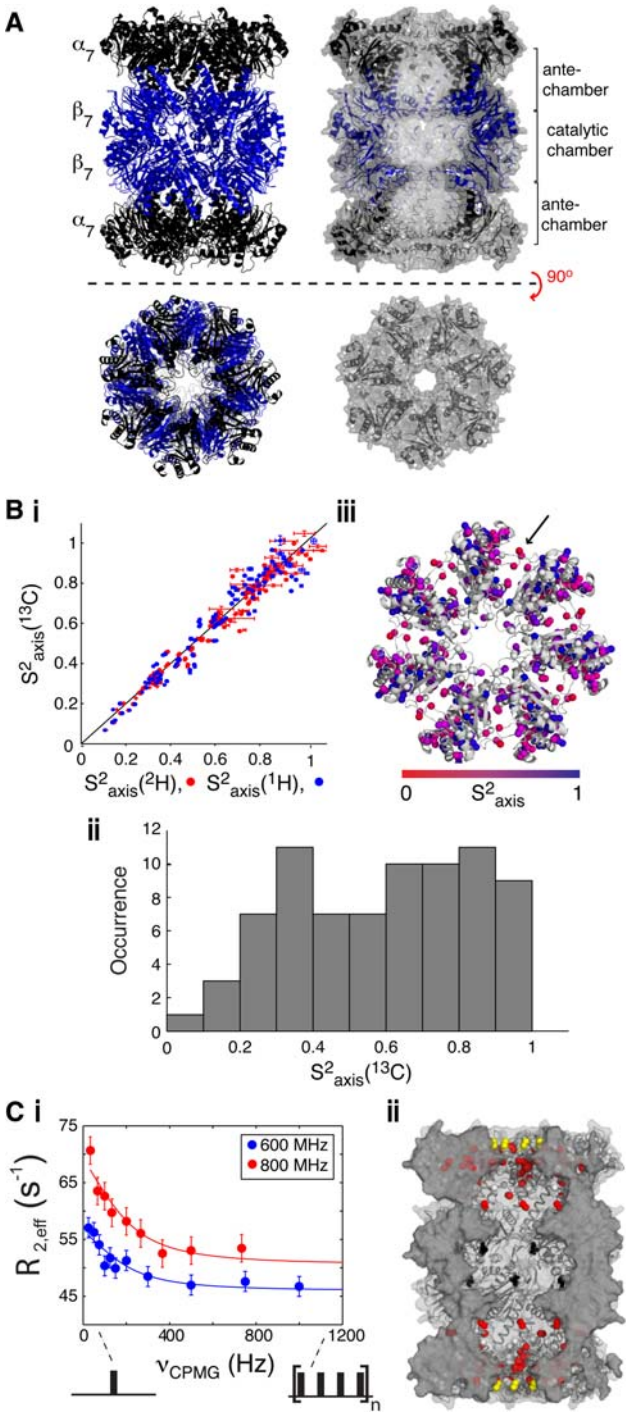

Fig. 3 Dynamics of the proteasome (Sprangers and Kay 2007b). **a** ▶ Structure of the proteasome (Forster et al. 2005; Lowe et al. 1995) shown in cartoon (*left*) and space filling (*right*) representations (PDB 1PMA). The proteasome is constructed from two protein precursors α and β, which are arranged as four stacked concentric heptameric rings with the indicated subunit compositions. These rings form three cavities—a catalytic chamber and two antechambers—that are located at the interface between adjacent rings. **b** Measurement of the order parameter S^2_{axis} quantifying nanosecond dynamics. (*i*) Correlation between S^2_{axis} values obtained using ^{13}C, ^{2}H, and ^{1}H probes attached to Ile, Leu and Val methyl groups in the 'half-proteasome construct' $\alpha_7\alpha_7$. The correlation between $S^2_{\text{axis}}(^{13}\text{C})$ and $S^2_{\text{axis}}(^{2}\text{H})$ is in red ($R = 0.96$), with the corresponding correlation between $S^2_{\text{axis}}(^{13}\text{C})$ and $S^2_{\text{axis}}(^{1}\text{H})$ in blue ($R = 0.95$). For reference a line $y = x$ is shown (*black*, *solid*). (*ii*) Histogram of S^2_{axis} values for methyl groups from Ile(δ1), Leu and Val in $\alpha_7\alpha_7$, indicating a wide range of mobilities. (*iii*) Position-dependent values of S^2_{axis}. A single α-ring is shown where the methyl groups of Ile(δ1), Leu and Val are represented by *spheres* and *colored* according to the value of S^2_{axis}. The flexible region between alpha subunits is designated by an *arrow*. **c** Measurement of millisecond methyl dynamics using methyl-TROSY based CPMG relaxation dispersion experiments. (*i*) Representative dispersion profiles obtained at two static magnetic fields. (*ii*) Position-dependent millisecond motions of methyl groups in the alpha ring of the proteasome. Locations of methyls undergoing concerted millisecond motion are indicated by *red* and *yellow* spheres, while active site residues (Thr 1) in the catalytic chamber are shown in *dark blue*. Sections of this figure have been adapted from Sprangers and Kay (2007b)

(Blobel and Dobberstein 1975), the mechanism by which this process occurs, and the molecular basis by which different signaling sequences that have no primary sequence homology are able to bind to SecA with high fidelity (von Heijne 1985), has remained poorly understood. In a seminal contribution Kalodimos and coworkers have exploited the Methyl-TROSY effect in studies to (1) determine the solution structure of a signal peptide bound to SecA, (2) to provide a molecular mechanism for inhibition of signal peptide binding by the C tail of the enzyme and (3) to show that the protein exists in dynamic equilibrium between a pair of alternate conformations in solution (Gelis et al. 2007).

SecA is a 200 kDa complex comprising two identical subunits containing several independently folded subdomains, Fig. 4a. As in the NMR studies involving ATCase and the 20S CP proteasome, discussed above, SecA was produced with U-^{2}H, Ile-[$\delta1^{13}CH_3$], Leu,Val-[$^{13}CH_3$,$^{12}CD_3$]-labeling, however, $^{13}CH_3$-Met was added additionally to the growth medium to generate further reporter groups. The resulting ^{13}C–^{1}H HMQC spectrum of SecA is of high quality, with the majority of cross-peaks assigned based on a strategy which includes (1) 'divide-and-conquer' in which smaller fragments of SecA were assigned followed by assignment transfer to the intact complex by comparison of 2D HMQC and 3D NOESY data sets and (2) mutagenesis (Gelis et al. 2007), Fig. 4bi–iv.

Nitroxide spin labels were introduced into both the N- and C-terminal regions of the SecA LamB signal peptide (one at a time) and its binding site on SecA determined from paramagnetic relaxation enhancement experiments (Battiste and Wagner 2000; Clore and Iwahara 2009) by comparing methyl HMQC spectra of the complex with either oxidized or reduced spin-label. In addition, the bound conformation of the peptide was established by Transfer NOE experiments (Ni 1994); together with the nitroxide data a structure of the complex was calculated, Fig. 4c. The signal peptide binds into a large groove formed at the interface between the PBD

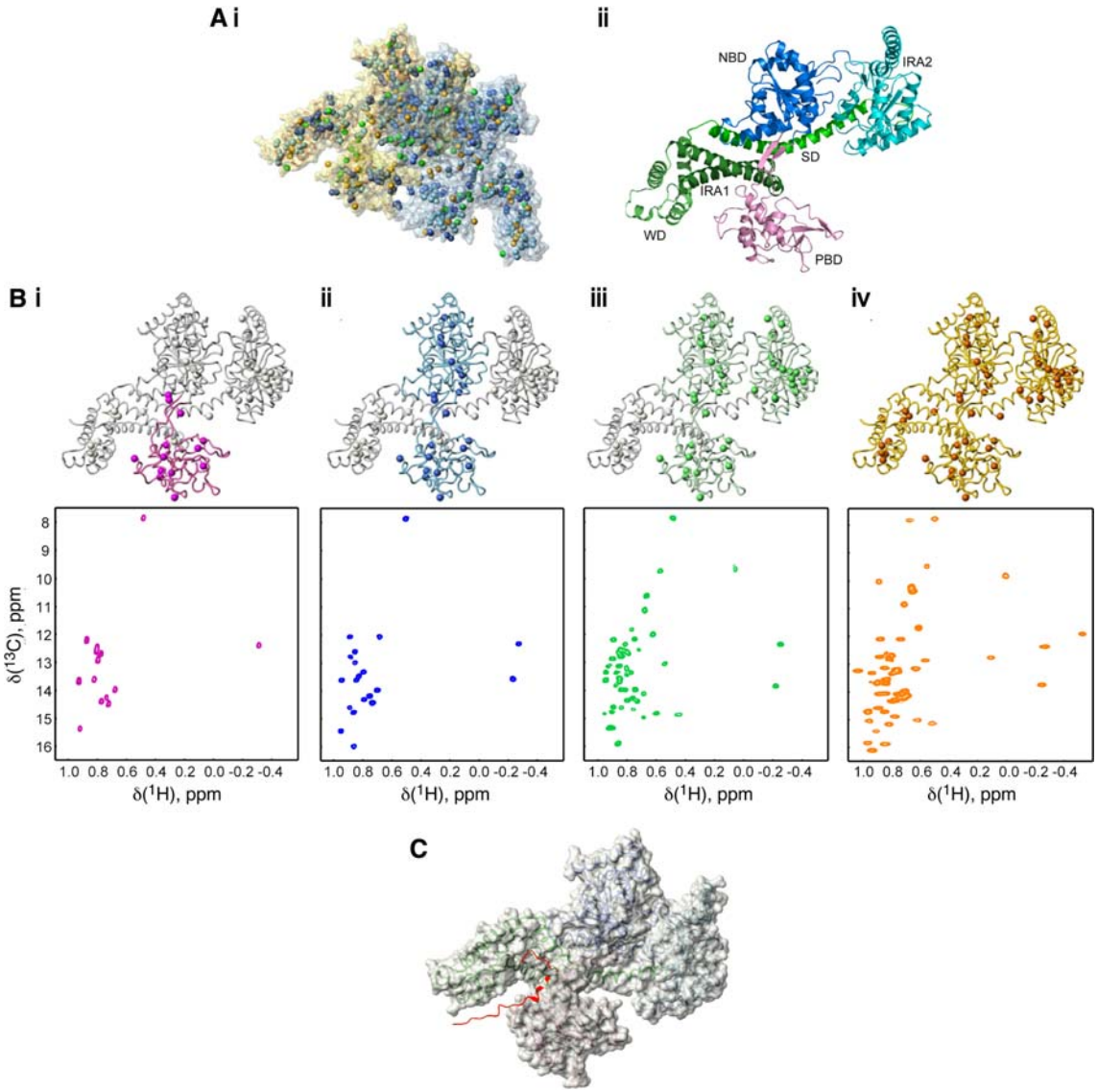

Fig. 4 Binding of signal peptides to SecA (Gelis et al. 2007). **a** SecA is composed of two identical subunits, represented as *yellow* and *blue* transparent surfaces, respectively. (*i*) Locations of methyl groups, indicated by *spheres*, with *colors* signifying the type of amino acid from which each methyl is derived (Ile, *orange*; Leu, *light blue*; Val, *dark blue*; Met, *green*). (*ii*) Structure of one of the subunits of SecA, shown in cartoon representation and *colored* by domain. **b** Assignment of ^{13}C–^{1}H HMQC spectra was achieved by labeling only one or a series of domains. Regions labeled are indicated in the context of the monomer structure, with Ile $\delta 1$ methyl groups shown as *colored spheres*. Increasing regions of the structure are labeled from *left* to *right*. **c** Structure of the LamB signal peptide (*red*) bound to SecA. Adapted from Gelis et al. (2007)

and IRA1 domains (Fig. 4aii) and is stabilized by both electrostatic interactions involving its positively charged N-terminus and the negatively charged SecA binding surface as well as hydrophobic contacts between the peptide α-helix and the binding interface. Moreover, the binding groove is large and plastic so that a range of targets can be accommodated. A remarkable aspect of the structure is that a C-terminal zinc-finger domain partially occludes the binding site, decreasing the affinity of the LamB peptide binding interaction by an order of magnitude relative to the case where the SecA tail is removed. Notably, binding of another factor, SecB, to the complex removes the auto-inhibition. It is suggested that this inhibition plays a role in ensuring the fidelity of the peptide–SecA interaction that would only occur upon formation of the ternary complex with SecB (Gelis et al. 2007).

Looking towards the future

The development of robust methods for the production of ^{1}H,^{13}C methyl-labeled, highly deuterated proteins in

concert with experiments that exploit the methyl-TROSY effect has facilitated the study of a number of very high molecular weight proteins. Included in the list are the 120 kDa CheA-CheW complex (Hamel and Dahlquist 2005), the 240 kDa Arp2/3 complex (Kreishman-Deitrick et al. 2005), a 300 kDa fragment of AAA-ATPase p97 (Isaacson et al. 2007), the 300 kDa ClpP protease at temperatures as low as 0.5°C (Sprangers et al. 2005) and the 490 kDa TET2 aminopeptidase (Amero et al. 2009), in addition to the 200 kDa SecA translocase (Gelis et al. 2007), the 300 kDa aspartate transcarbamoylase (Velyvis et al. 2007), and the 670 kDa 20S CP proteasome (Sprangers and Kay 2007b), both without and with the 11S activator complex (1.0 MDa), that have been highlighted above. The preceding discussion establishes that quantitative information—in terms of dynamics, structure and function—is beginning to emerge from these studies.

Despite a number of very interesting applications to date, it is easy to envision improvements to the 'methyl strategy' at almost all levels. From the labeling side it would be advantageous in at least some applications to have available pure pro-S and pure pro-R Leu/Val precursor. Proteins produced from the chemically pure compound would give rise to Leu/Val spectra with double the sensitivity, stereo-specific assignments would be available de facto, and spectra would be simplified relative to those produced by a protein generated from a 50–50 mixture of stereo-isomers. Of course, a pair of samples (pro-R, pro-S) would be needed, increased spectrometer time would be required and the cost per sample would be significantly elevated since the production of the appropriate precursors would be expensive. Nevertheless, it is anticipated that the advantages would be considerable in studies of large molecular machines where resolution and sensitivity can be critical.

Improvements to the basic methyl-TROSY pulse scheme, HMQC, are already occurring, with the development of SOFAST HMQC methodology (Schanda et al. 2005) which maximizes the signal-to-noise per unit measuring time. This is achieved by optimizing the excitation pulse in the HMQC sequence to an angle set according to the Ernst relation (Ernst et al. 1987). A second, much smaller gain for highly deuterated, methyl protonated proteins, is achieved by using a methyl selective excitation pulse so that residual, non-methyl protons (in practice a few percent for deuterated proteins) are positioned along the $+Z$-axis prior to acquisition and hence act as a reservoir of magnetization, increasing the effective relaxation rates of methyl spins by cross-relaxation (Pervushin et al. 2002). The utility of this method was demonstrated in a spectacular fashion by recording quite reasonable ^{13}C–^{1}H HMQC spectra in only 3 s on samples of U-^{15}N,^{12}C,^{2}H Ile-[$\delta1^{13}CH_3$] and U-^{15}N,^{12}C,^{2}H Ala-[$\beta^{13}CH_3$] TET2, a 468 kDa aminopeptidase (Amero et al. 2009). This opens up the possibility of monitoring kinetic processes at a residue-specific level in real time, providing yet another important application for this methodology.

Currently a major bottleneck in studies of very high molecular weight particles is obtaining methyl group assignments, but there are indications that this may change in the near future. To this point, the domain parsing, 'divide-and-conquer' strategy is a laborious, but nevertheless important component of the process by which residue specific assignments are made. Recently an automated method was developed for assigning spectra using as input an X-ray structure, a ^{13}C–^{1}H HMQC data set, 3D NOESY and methyl through-bond correlation spectra. Using this algorithm accurate assignments were obtained for well over 90% of the 93 Ile, Leu, Val methyl correlations in the HMQC spectrum of the $\alpha_7\alpha_7$ half-proteasome particle (Xu et al. 2009). Other, complementary, approaches for generating methyl group assignments are also possible. The addition of paramagnetic metal ions/tags to proteins leads to peak broadening that depends on the distance between the paramagnet and the NMR spin of interest and/or changes in chemical shifts (pseudocontact shifts, PCSs) that are a function of both the orientation and the length of the vector connecting the unpaired electron with the NMR spin (Bertini et al. 2005). Experimentally derived relaxation enhancements can be compared with those predicted from an X-ray structure and matches in predicted/measured rates used to assist with assignment. Potentially even more powerful is a comparison of calculated and measured PCSs, although the computation of PCSs requires both an X-ray structure of the protein and a handful of assignments ($\geq$5) from which a magnetic susceptibility tensor can be generated. Otting and coworkers have used a comparison of PCS values in the assignment of methyl groups in a 30 kDa protein complex from DNA polymerase III (John et al. 2007), with chemical shifts calculated on the basis of a high quality susceptibility tensor generated from ^{15}N data. Preliminary indications are that this approach will be very powerful in studies of supra-molecular systems as well, even if only a handful of methyl group assignments are available initially from which to calculate a susceptibility tensor.

It is clear that methyl labeling methods along with simple spectroscopy optimized to preserve long-lived methyl coherences have greatly extended the size of protein complexes that can be studied by NMR and that insight into a wide range of important biochemical problems can be obtained using methyl group probes. Additional advances in labeling methodology, combined with novel pulse sequences and technological improvements in instrumentation, will further increase the scope of systems and types of questions that can be addressed by NMR measurements.

Acknowledgments This work was supported by a grant from the Canadian Institutes of Health Research. The authors are grateful to Prof. Babis Kalodimos, Rutgers University, for kindly providing the materials for Fig. 4. L. E. K. holds a Canada Research Chair in Biochemistry.

References

Adams J (2004) The proteasome: a suitable antineoplastic target. Nat Rev Cancer 4:349–360

Amero C, Schanda P, Dura MA, Ayala I, Marion D, Franzetti B, Brutscher B, Boisbouvier J (2009) Fast two-dimensional NMR spectroscopy of high molecular weight protein assemblies. J Am Chem Soc 131:3448–3449

Ayala I, Sounier R, Use N, Gans P, Boisbouvier J (2009) An efficient protocol for the complete incorporation of methyl-protonated alanine in perdeuterated protein. J Biomol NMR 43:111–119

Battiste JL, Wagner G (2000) Utilization of site-directed spin labeling and high-resolution heteronuclear nuclear magnetic resonance for global fold determination of large proteins with limited nuclear overhauser effect data. Biochemistry 39:5355–5365

Bax A (1994) Multidimensional nuclear magnetic resonance methods for protein studies. Curr Opin Struct Biol 4:738–744

Bertini I, Luchinat C, Parigi G, Pierattelli R (2005) NMR spectroscopy of paramagnetic metalloproteins. Chembiochem 6:1536–1549

Blobel G, Dobberstein B (1975) Transfer of proteins across membranes. I. Presence of proteolytically processed and unprocessed nascent immunoglobulin light chains on membrane-bound ribosomes of murine myeloma. J Cell Biol 67:835–851

Cheng Y (2009) Toward an atomic model of the 26S proteasome. Curr Opin Struct Biol 19:203–208

Clore GM, Gronenborn AM (1991) Structures of larger proteins in solution: three- and four-dimensional heteronuclear NMR spectroscopy. Science 252:1390–1399

Clore GM, Iwahara J (2009) Theory, practice, and applications of paramagnetic relaxation enhancement for the characterization of transient low-population states of biological macromolecules and their complexes. Chem Rev 109:4108–4139

Crespi HL, Rosenberg RM, Katz JJ (1968) Proton magnetic resonance of proteins fully deuterated except for ^{1}H-leucine side-chains. Science 161:795–796

Driessen AJ, Brundage L, Hendrick JP, Schiebel E, Wickner W (1991) Preprotein translocase of *Escherichia coli*: solubilization, purification, and reconstitution of the integral membrane subunits SecY/E. Methods Cell Biol 34:147–165

Economou A, Wickner W (1994) SecA promotes preprotein translocation by undergoing ATP-driven cycles of membrane insertion and deinsertion. Cell 78:835–843

Eisenstein E, Markby DW, Schachman HK (1990) Heterotropic effectors promote a global conformational change in aspartate transcarbamoylase. Biochemistry 29:3724–3731

Ernst RR, Bodenhausen G, Wokaun A (1987) Principles of nuclear magnetic resonance in one and two dimensions. Oxford University Press, Oxford

Fiaux J, Bertelsen EB, Horwich AL, Wuthrich K (2002) NMR analysis of a 900K GroEL GroES complex. Nature 418:207–211

Fischer M, Kloiber K, Hausler J, Ledolter K, Konrat R, Schmid W (2007) Synthesis of a 13C-methyl-group-labeled methionine precursor as a useful tool for simplifying protein structural analysis by NMR spectroscopy. Chembiochem 8:610–612

Forster A, Masters EI, Whitby FG, Robinson H, Hill CP (2005) The 1.9 A structure of a proteasome-11S activator complex and implications for proteasome-PAN/PA700 interactions. Mol Cell 18:589–599

Gardner KH, Kay LE (1997) Production and incorporation of ^{15}N, ^{13}C, ^{2}H (^{1}H-δ1 methyl) isoleucine into proteins for multidimensional NMR studies. J Am Chem Soc 119:7599–7600

Gardner KH, Rosen MK, Kay LE (1997) Global folds of highly deuterated, methyl protonated proteins by multidimensional NMR. Biochemistry 36:1389–1401

Gelis I, Bonvin AM, Keramisanou D, Koukaki M, Gouridis G, Karamanou S, Economou A, Kalodimos CG (2007) Structural basis for signal-sequence recognition by the translocase motor SecA as determined by NMR. Cell 131:756–769

Goto NK, Kay LE (2000) New developments in isotope labeling strategies for protein solution NMR spectroscopy. Curr Opin Struct Biol 10:585–592

Goto NK, Gardner KH, Mueller GA, Willis RC, Kay LE (1999) A robust and cost-effective method for the production of Val, Leu, Ile (δ1) methyl-protonated 15N-, 13C-, 2H-labeled proteins. J Biomol NMR 13:369–374

Gross JD, Gelev VM, Wagner G (2003) A sensitive and robust method for obtaining intermolecular NOEs between side chains in large protein complexes. J Biomol NMR 25:235–242

Grzesiek S, Anglister J, Ren H, Bax A (1993) 13C line narrowing by 2H decoupling in 2/13C/15N-enriched proteins. Applications to triple resonance 4D J-connectivity of sequential amides. J Am Chem Soc 115:4369–4370

Hajduk PJ, Augeri DJ, Mack J, Mendoza R, Yang JG, Betz SF, Fesik SW (2000) NMR-based screening of proteins containing C-13 labeled methyl groups. J Am Chem Soc 122:7898–7904

Hamel DJ, Dahlquist FW (2005) The contact interface of a 120 kD CheA-CheW complex by methyl TROSY interaction spectroscopy. J Am Chem Soc 127:9676–9677

Ikura M, Kay LE, Bax A (1990) A novel approach for sequential assignment of 1H, 13C, and 15N spectra of proteins: heteronuclear triple-resonance three-dimensional NMR spectroscopy. Application to calmodulin. Biochemistry 29:4659–4667

Isaacson RL, Simpson PJ, Liu M, Cota E, Zhang X, Freemont P, Matthews S (2007) A new labeling method for methyl transverse relaxation-optimized spectroscopy NMR spectra of alanine residues. J Am Chem Soc 129:15428–15429

Janin J, Miller S, Chothia C (1988) Surface, subunit interfaces and interior of oligomeric proteins. J Mol Biol 204:155–164

John M, Schmitz C, Park AY, Dixon NE, Huber T, Otting G (2007) Sequence-specific and stereospecific assignment of methyl groups using paramagnetic lanthanides. J Am Chem Soc 129:13749–13757

Kainosho M, Torizawa T, Iwashita Y, Terauchi T, Mei Ono A, Guntert P (2006) Optimal isotope labelling for NMR protein structure determinations. Nature 440:52–57

Kay LE, Ikura M, Tschudin R, Bax A (1990) Three-dimensional triple-resonance NMR spectroscopy of isotopically enriched proteins. J Magn Reson 89:496–514

Kobayashi M, Yagi H, Yamazaki T, Yoshida M, Akutsu H (2008) Dynamic inter-subunit interactions in thermophilic F(1)-ATPase subcomplexes studied by cross-correlated relaxation-enhanced polarization transfer NMR. J Biomol NMR 40:165–174

Korzhnev DM, Kloiber K, Kanelis V, Tugarinov V, Kay LE (2004) Probing slow dynamics in high molecular weight proteins by methyl-TROSY NMR spectroscopy: application to a 723-residue enzyme. J Am Chem Soc 126:3964–3973

Kreishman-Deitrick M, Goley ED, Burdine L, Denison C, Egile C, Li R, Murali N, Kodadek TJ, Welch MD, Rosen MK (2005) NMR analyses of the activation of the Arp2/3 complex by neuronal Wiskott–Aldrich syndrome protein. Biochemistry 44:15247–15256

LeMaster DM, Richards FM (1988) NMR sequential assignment of *Escherichia coli* thioredoxin utilizing random fractional deuteration. Biochemistry 27:142–150

Lichtenecker R, Ludwiczek ML, Schmid W, Konrat R (2004) Simplification of protein NOESY spectra using bioorganic precursor synthesis and NMR spectral editing. J Am Chem Soc 126:5348–5349

Lipscomb WN (1994) Aspartate transcarbamylase from *Escherichia coli*: activity and regulation. Adv Enzymol Relat Areas Mol Biol 68:67–151

Lowe J, Stock D, Jap B, Zwickl P, Baumeister W, Huber R (1995) Crystal structure of the 20S proteasome from the archaeon *T. acidophilum* at 3.4 Å resolution. Science 268:533–539

Mao X, Li X, Sprangers R, Wang X, Venugopal A, Wood T, Zhang Y, Kuntz DA, Coe E, Trudel S, Rose D, Batey RA, Kay LE, Schimmer AD (2009) Clioquinol inhibits the proteasome and displays preclinical activity in leukemia and myeloma. Leukemia 23:585–590

Marion D, Driscoll PC, Kay LE, Wingfield PT, Bax A, Gronenborn AM, Clore GM (1989) Overcoming the overlap problem in the assignment of 1H NMR spectra of larger proteins by use of three-dimensional heteronuclear 1H–15N Hartmann–Hahn-multiple quantum coherence and nuclear Overhauser-multiple quantum coherence spectroscopy: application to interleukin 1β. Biochemistry 28:6150–6156

Markley JL, Putter I, Jardetzky O (1968) High resolution nuclear magnetic resonance spectra of selectively deuterated staphylococcal nuclease. Science 161:1249–1251

Matsumoto G, Yoshihisa T, Ito K (1997) SecY and SecA interact to allow SecA insertion and protein translocation across the *Escherichia coli* plasma membrane. EMBO J 16:6384–6393

Metzler WJ, Wittekind M, Goldfarb V, Mueller L, Farmer BT (1996) Incorporation of 1H/13C/15N-{Ile, Leu, Val} into a perdeuterated, 15N-labeled protein: potential in structure determination of large proteins by NMR. J Am Chem Soc 118:6800–6801

Monod J, Wyman J, Changeux JP (1965) On the nature of allosteric transitions: a plausible model. J Mol Biol 12:88–118

Montelione GT, Wagner G (1990) Conformation-independent sequential NMR connections in isotope-enriched peptides by H–1C–13–N15 triple resonance experiments. J Magn Reson 87: 183–188

Ni F (1994) Recent developments in transferred NOE methods. Prog Nucl Magn Reson Spectrosc 26:517–606

Nicholson LK, Kay LE, Baldisseri DM, Arango J, Young PE, Bax A, Torchia DA (1992) Dynamics of methyl groups in proteins as studied by proton-detected 13C NMR spectroscopy. Application to the leucine residues of staphylococcal nuclease. Biochemistry 31:5253–5263

Ottiger M, Delaglio F, Bax A (1998) Measurement of J and dipolar couplings from simplified two-dimensional NMR spectra. J Magn Reson 131:373–378

Pervushin K, Riek R, Wider G, Wüthrich K (1997) Attenuated T_2 relaxation by mutual cancellation of dipole–dipole coupling and chemical shift anisotropy indicates an avenue to NMR structures of very large biological macromolecules in solution. Proc Natl Acad Sci USA 94:12366–12371

Pervushin K, Vogeli B, Eletsky A (2002) Longitudinal (1)H relaxation optimization in TROSY NMR spectroscopy. J Am Chem Soc 124:12898–12902

Pickart CM, Cohen RE (2004) Proteasomes and their kin: proteases in the machine age. Nat Rev Mol Cell Biol 5:177–187

Rabl J, Smith DM, Yu Y, Chang SC, Goldberg AL, Cheng Y (2008) Mechanism of gate opening in the 20S proteasome by the proteasomal ATPases. Mol Cell 30:360–368

Rosen MK, Gardner KH, Willis RC, Parris WE, Pawson T, Kay LE (1996) Selective methyl group protonation of perdeuterated proteins. J Mol Biol 263:627–636

Sattler M, Schleucher J, Griesinger C (1999) Heteronuclear multidimensional NMR experiments for the structure determination of proteins in solution employing pulsed field gradients. Prog Nucl Magn Reson Spectrosc 34:93–158

Schachman HK (1988) Can a simple model account for the allosteric transition of aspartate transcarbamoylase? J Biol Chem 263: 18583–18586

Schanda P, Kupce E, Brutscher B (2005) SOFAST-HMQC experiments for recording two-dimensional heteronuclear correlation spectra of proteins within a few seconds. J Biomol NMR 33: 199–211

Shan X, Gardner KH, Muhandiram DR, Rao NS, Arrowsmith CH, Kay LE (1996) Assignment of ^{15}N, ^{13}Cα, ^{13}Cβ and HN resonances in an ^{15}N, ^{13}C, ^{2}H labeled 64 kDa trp repressor-operator complex using triple resonance NMR spectroscopy and ^{2}H-decoupling. J Am Chem Soc 118:6570–6579

Spirin AS, Baranov VI, Ryabova LA, Ovodov SY, Alakhov YB (1988) A continuous cell-free translation system capable of producing polypeptides in high yield. Science 242:1162–1164

Sprangers R, Kay LE (2007a) Probing supramolecular structure from measurement of methyl (1)H–(13)C residual dipolar couplings. J Am Chem Soc 129:12668–12669

Sprangers R, Kay LE (2007b) Quantitative dynamics and binding studies of the 20S proteasome by NMR. Nature 445:618–622

Sprangers R, Gribun A, Hwang PM, Houry WA, Kay LE (2005) Quantitative NMR spectroscopy of supramolecular complexes: dynamic side pores in ClpP are important for product release. Proc Natl Acad Sci USA 102:16678–16683

Sprangers R, Li X, Mao X, Rubinstein JL, Schimmer AD, Kay LE (2008) TROSY-based NMR evidence for a novel class of 20S proteasome inhibitors. Biochemistry 47:6727–6734

Stryer L (1995) Biochemistry, 4th edn. W. H. Freeman and Company, New York

Tauc P, Leconte C, Kerbiriou D, Thiry L, Herve G (1982) Coupling of homotropic and heterotropic interactions in *Escherichia coli* aspartate transcarbamylase. J Mol Biol 155:155–168

Thiry L, Herve G (1978) The stimulation of *Escherichia coli* aspartate transcarbamylase activity by adenosine triphosphate. Relation with the other regulatory conformational changes; a model. J Mol Biol 125:515–534

Tugarinov V, Kay LE (2003a) Ile, Leu, and Val methyl assignments of the 723-residue malate synthase G using a new labeling strategy and novel NMR methods. J Am Chem Soc 125:13868–13878

Tugarinov V, Kay LE (2003b) Side chain assignments of Ile delta 1 methyl groups in high molecular weight proteins: an application to a 46 ns tumbling molecule. J Am Chem Soc 125:5701–5706

Tugarinov V, Kay LE (2004) An isotope labeling strategy for methyl TROSY spectroscopy. J Biomol NMR 28:165–172

Tugarinov V, Kay LE (2005a) Methyl groups as probes of structure and dynamics in NMR studies of high-molecular-weight proteins. Chembiochem 6:1567–1577

Tugarinov V, Kay LE (2005b) Quantitative 13C and 2H NMR relaxation studies of the 723-residue enzyme malate synthase G reveal a dynamic binding interface. Biochemistry 44:15970–15977

Tugarinov V, Hwang P, Ollerenshaw J, Kay LE (2003) Cross-correlated relaxation enhanced 1H–13C NMR spectroscopy of methyl groups in very high molecular weight proteins and protein complexes. J Am Chem Soc 125:10420–10428

Tugarinov V, Hwang PM, Kay LE (2004) Nuclear magnetic resonance spectroscopy of high-molecular-weight proteins. Annu Rev Biochem 73:107–146

Tugarinov V, Sprangers R, Kay LE (2007) Probing side-chain dynamics in the proteasome by relaxation violated coherence transfer NMR spectroscopy. J Am Chem Soc 129:1743–1750

Velyvis A, Yang YR, Schachman HK, Kay LE (2007) A solution NMR study showing that active site ligands and nucleotides

directly purturb the allosteric equilibrium in aspartate transcarbamolyase. Proc Natl Acad Sci USA 104:8815–8820

Velyvis A, Schachman HK, Kay LE (2009) Application of methyl-TROSY NMR to test allosteric models describing effects of nucleotide binding to aspartate transcarbamoylase. J Mol Biol 387:540–547

von Heijne G (1985) Signal sequences: the limits of variation. J Mol Biol 184:99–105

Wang L, Miller A, Kendall DA (2000) Signal peptide determinants of SecA binding and stimulation of ATPase activity. J Biol Chem 275:10154–10159

Xu Y, Liu M, Simpson PJ, Isaacson R, Cota E, Marchant J, Yang D, Zhang X, Freemont P, Matthews S (2009) Automated assignment in selectively methyl-labeled proteins. J Am Chem Soc 131:9480–9481

Yamazaki T, Lee W, Arrowsmith CH, Muhandiram DR, Kay LE (1994) A suite of triple resonance NMR experiments for the backbone assignment of ^{15}N, ^{13}C, ^{2}H labeled proteins with high sensitivity. J Am Chem Soc 116:11655–11666

Yang D, Nagayama K (1996) A sensitivity-enhanced method for measuring heteronuclear long-range coupling constants from the displacement of signals in two 1D subspectra. J Magn Reson Ser A 118:117–121

Zheng D, Huang YJ, Moseley HN, Xiao R, Aramini J, Swapna GV, Montelione GT (2003) Automated protein fold determination using a minimal NMR constraint strategy. Protein Sci 12:1232–1246